journal of the mechanical behavior of biomedical materials 160 (2024) 106720

Contents lists available at ScienceDirect

Journal of the Mechanical Behavior of Biomedical Materials

journal homepage: www.elsevier.com/locate/jmbbm

Biomechanical simulation of segmented intrusion of a mandibular canine using Robot Orthodontic Measurement & Simulation System (ROSS)

Hisham Sabbagh *, Benedikt Dotzer, Uwe Baumert, Linus Hötzel, Corinna Lesley Seidel, Andrea Wichelhaus

LMU University Hospital, Department of Orthodontics and Dentofacial Orthopedics, Goethesstrasse 70, Munich, Germany

ARTICLE INFO

Keywords:
Biomechanics
Orthodontics
3D measurement
Force-control
Robotics
Segmented intrusion
Segmented arch mechanics

ABSTRACT

Objective: Aim of this study was to investigate the forces and moments during segmented intrusion of a mandibular canine using Cantilever-Intrusion-Springs (CIS).

Methods: Three different CIS modifications were investigated using a robotic biomechanical simulation system: unmodified CIS (#1, control), CIS with a lingual directed 6° toe-in bend (#2), and CIS with an additional 20° twist bend (#3). Tooth movement was simulated by the apparative robotic stand, controlled by a force-control algorithm, recording the acting forces and moments with a force-torque sensor. Statistical analysis was performed using Shapiro-Wilk, Kolmogorov-Smirnov, Kruskal-Wallis ANOVA and post hoc tests with Bonferroni correction ($\alpha = 0.05$).

Results: The initial intrusive force, which was uniformly generated by a 35° Tip-Back bend, decreased significantly ($p < 0.05$) from 0.31 N in group (#1) to 0.28 N in group (#3). Vestibular crown tipping reduced significantly ($p < 0.05$) from 2.11° in group (#1) and 1.72° in group (#2) to 0.05° in group (#3). Matching to that the direction of orovestibular force significantly ($p < 0.05$) shifted from 0.15 N to vestibular in group (#1) to 0.51 N to oral in group (#3) and the orovestibular tipping moment decreased also significantly ($p < 0.05$) from 4.63 Nmm to vestibular in group (#1) to 3.56 Nmm in group (#2) and reversed to 1.20 Nmm to oral in group (#3). Apart from that the orovestibular displacement changed significantly ($p < 0.05$) from 0.66 mm in buccal direction in group (#1) to 0.29 mm orally in group (#2) and 1.49 mm in oral direction as well in group (#3).

Significance: None of the modifications studied achieved pure mandibular canine intrusion without collateral effects. The significant lingual displacement caused by modification (#3) is, not least from an aesthetic perspective, considered much more severe than a slight tipping of the canine. Consequently, modification (#2) can be recommended for clinical application based on the biomechanical findings.

1. Introduction

Deep bite malocclusions are defined by an excessive vertical overlap of the upper and lower incisors of more than 2–3 mm or one third of the clinical crown (Nanda and Kuhlberg, 2007). The global distribution of deep bite malocclusions were found to range between 24.34% in the mixed dentition and 20.14% in the permanent dentition (Proffit et al., 2007; Alhammadi et al., 2018). The unfavourable consequences of this type of malocclusion, such as predisposition to periodontal issues, abnormal function, improper chewing, excessive stress, trauma, functional difficulties, bruxism, clenching, and disturbances in the temporomandibular joint, necessitating treatment to align the bite and prevent further complications (Agrawal, 2016). The orthodontic treatment approach depends on aetiology, severity, age and detention state of the patient (Ghafari et al., 2013). In general, orthodontic correction of deep bite malocclusions and overbite reduction includes extrusion of the posterior teeth, intrusion of the anterior teeth or a combination of both (Parker et al., 1995). In children and adolescent patients, passive extrusion of the posterior teeth and relative intrusion of the incisors can be achieved using functional orthodontic appliances or bite blocks with good long-term stability (Proffit et al., 2007; Wichelhaus et al., 2003). In adult patients with permanent dentition, extrusion of the posterior teeth was shown to be less stable, given the completion of vertical growth of the mandibular ramus and relapse due to the masticatory forces (Sankey et al., 2000; Otto et al., 1980; Al-Buraiki et al., 2005). Therefore, orthodontic intrusion of canines and incisors is commonly performed to

* Corresponding author.
E-mail address: hisham.sabbagh@med.uni-muenchen.de (H. Sabbagh).

https://doi.org/10.1016/j.jmbbm.2024.106720
Received 6 May 2024; Received in revised form 21 August 2024; Accepted 3 September 2024
Available online 6 September 2024
1751-6161/© 2024 The Authors. Published by Elsevier Ltd. This is an open access article under the CC BY license (http://creativecommons.org/licenses/by/4.0/).

reduce overbite (Baccetti et al., 2012). In general, tooth intrusion can be performed using removable or fixed appliances (Abu Arqub et al., 2023). In adults with pronounced deep bite malocclusions and extruded incisors, segmented intrusion with fixed appliances is recommended, as this technique enables precise control of the applied force system (Burstone, 1966). In addition to the upper and lower incisors, mandibular canines are extruded in 50 % of patients with increased overbite (Ricketts et al., 1979). Due to the fact that simultaneous orthodontic intrusion of all six anterior teeth can have multiple adverse repercussions, especially in the posterior anchorage unit, segmented intrusion of single teeth offers a much more efficient therapy option. To intrude both the front and canine teeth together, a force of approximately 100 cN would be required; however, this would lead to a rotational moment of 3000 cN-mm in the posterior segment of the side tooth region, causing the tipping of the side teeth to occur faster than the intrusion of the front and canine teeth, rendering this intrusion mechanic ineffective and impractical (Burstone, 1977). In contrast, separate segmented intrusion of the lower canines offers advantages in terms of efficiency and handling. For this segmented intrusion the use of cantilever intrusion springs (CIS) was proposed, due to their advantageous properties for controlling the biomechanics of tooth movement and the theoretically possible application of force through the center of resistance, thereby achieving pure intrusion (Burstone, 1977). Only three available studies investigated biomechanical aspects of canine intrusion (Caballero et al., 2015; Thote et al., 2017a, 2017b). Caballero et al. investigated different CIS modifications using the finite element method (FEM). The baseline modification was made from a β-titanium sectional archwire with a 3 mm vertical loop and a 35° apical directed tip-back bend. The baseline modification was altered in terms of applied lingual directed toe-in bends of varying degrees. The authors concluded that the application of a 6° toe-in bend would result in pure canine intrusion with no collateral effects, in contrast to the baseline modification, which showed vestibular crown tipping (Caballero et al., 2015). Two similar FEM-studies investigated different modifications of the CIS, however using lingual fixed appliances. The results of their study also suggested that first-order bends are required to achieve pure intrusion of a mandibular canine (Thote et al., 2017a, 2017b). However, pure intrusion without collateral effects is unlikely to occur clinically according to biomechanical considerations. Although numerical methods such as the FEM are being increasingly utilized for biomechanical investigations and are based on experimentally determined parameters, they rely on simplified assumptions and are therefore limited in their predictive validity (Cicciu, 2020; Cervino et al., 2020). One advantage of FEM models is their adaptability and the ability to simulate the mechanical behaviours of biological tissue to a certain degree (Kamble et al., 2012; Singh et al., 2016; Luchian et al., 2021). However, these simulations depend on virtual representations of orthodontic appliances that can only reproduce the actual material behaviours to a certain extent (Romanyk et al., 2020; Zeno and Ammoury, 2023). Equipment based biomechanical test stands are less adaptable than digital models, but allow for the investigation of actual physical properties of orthodontic mechanics without subjective parameters and are thus suitable to verify silicon based calculations prior to clinical trials (Romanyk et al., 2020; Wanjun et al., 2015).

The study was carried out using an automated test stand based on a commercial six serial axis robotic system, which was equipped with a force-torque-sensor. A major innovation to previous research is the possibility to measure the dynamic course of forces and moments due to the principle of force-control, by calculating position corrections of the robot to cyclically reduce the forces and moments to a final position, where they either reach a minimum or come to zero. This process operates completely automatically, without manual adjustments during the experimental run. Therefore, it is possible to measure initially applied forces and moments and its changes during the experimental run. It is also possible to calculate the trajectory of the Center of Force as well as the Center of Resistance from the robot's geometrical data records. The aim of this study was to investigate the intrusion of a mandibular canine using the force-controled biomechanical test stand ROSS and to compare the effects of different modifications of CIS regarding their biomechanical behaviour. In particular, the extent of collateral effects associated with the different modifications during intrusion should be compared using the measured force-torque system during of simulated tooth movement. For the first time wird dabei das verhalten physischer Versuchsproben, anstatt digitaler Replikationen untersucht.

2. Materials and methods

2.1. Experimental setup

An experimental biomechanical test stand (ROSS) was used with a modified mandibular model and experimental tooth to investigate segmented orthodontic intrusion of a lower canine (Fig. 1) (Dotzer et al., 2023). The mandibular model was digitally created, based on a typodont model of a lower jaw using orthodontic imaging software (OnyxCeph^{3}™ Version 3.2.185; Image Instruments GmbH, Chemnitz, Germany). For reasons of mechanical integrity and reduced risk of fracturing the model was 3D-printed out of a titanium alloy (Ti6Al4V) using Direct Metal Laser Sintering (APWORKS GmbH, Taufkirchen, Germany). The area in which the intrusion of the lower canine should be examined was cut out from the titanium model using wire electro discharge machining (FANUC Robocut Alpha C400iA; FANUC K.K., Oshino, Japan). A corresponding typodont tooth, a lower left canine (tooth 33), was digitized using a desktop scanner (S300 Ortho; ZIRKONZAHN GmbH, Gais, Italy). An occlusal directed cylindrical recess with a diameter of 1.5 mm was incorporated into the base of the digital tooth model. Subsequently, the experimental tooth was 3D-printed using stereolithography (Grey Resin V4; Formlabs GmbH, Berlin, Germany). An M2 threaded bore was then screwed into the recess, allowing the tooth to be connected to the force-torque sensor's adapter plate via a corresponding threaded rod. The FTS Nano 17 SI-12-0.12 force-torque sensor (ATI Industrial Automation, USA), was mounted at the robot end effector and could measure forces along the three spatial axes with a resolution of 0.0031 N and moments with a accuracy of 0.0156 Nmm. Active self-ligating 0.022″ slot straightwire brackets with MBT prescription (Bioquick; Forestadent GmbH, Pforzheim, Germany) were bonded to the experimental model and the experimental tooth using a passive pre-bent 0.021" × 0.025″ steel archwire. The lower left premolars (teeth 34/35) were not bonded to simulate the application of segmented arch mechanics (Fig. 1).

2.2. Biomechanical simulation procedure and specimen

For the simulation of segmented intrusion of a mandibular canine, the tooth was extruded from its idealized position in the dental arch by 1.5 mm along its longitudinal axis, which corresponds to the vertical plane of the coordinate system. This misalignment was configured into the control software of the robot, allowing the tooth to be relocated to the identical starting position for the different simulation series. During the simulations, forces and moments generated by the intrusion springs were recorded by the sensor within its coordinate system. It was configured such to correspond with the orthodontic Tweed coordinate system, i.e. its x-axis corresponds to the mesiodistal axis, the y-axis corresponds to the orovestibular axis, and the z-axis corresponds to the vertical axis of the orthogonally aligned bracket (Fig. 2A). Consequently, a measured moment about the x-axis corresponds to an inclination moment, in the case of the y-axis to an angulation moment, and for the z-axis to a rotation moment. A positive F_z corresponds to an intrusive force, and a positive M_x corresponds to a protruding moment.

Mathematical corrections built into the control software ensured that distortions in measurement data caused by gravity or the robot's own weight could be excluded. Considering the measurement geometry, the recorded values were transformed to the force application point or

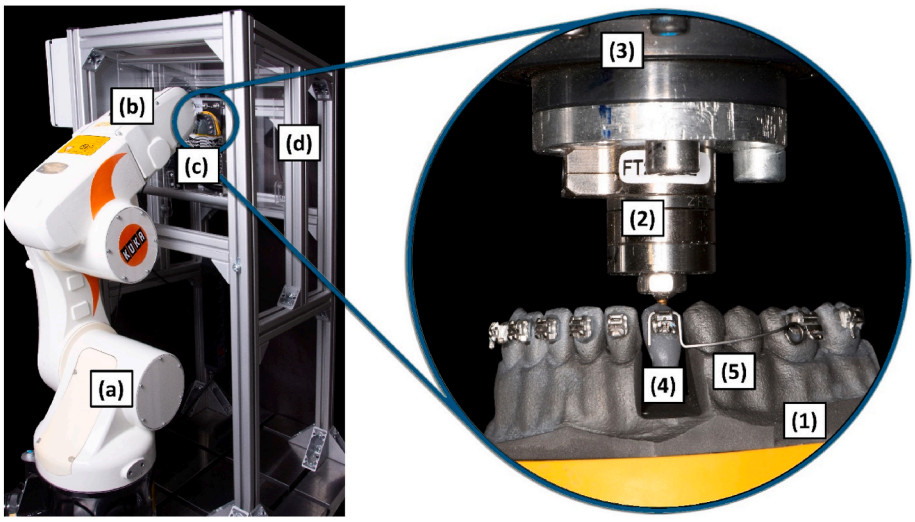

Fig. 1. ROSS: KUKA KR 5-sixx R650 Industrial robot (a), robot end effector with force-torque sensor and test tooth (b), KAVO Typodont model (c) within the reference frame constructed for the experiment including the thermal chamber (d). The Close-up shows further parts of the experimental setup: KAVO Typodont model made of high-strength titanium alloy (1), force-torque sensor (2), robot end effector (3), experimental tooth 33 (4) and active CIS (5).

Center of Force (CoF) and the Center of Resistance (CoR) of the tooth. This transformation was based on geometrical measurements of the distances and angles between the plane of the force/torque sensor and the CoF and CoR using 3D CAD software (Autodesk Inventor Professional, 2023; Autodesk Inc., San Rafael, USA) (Fig. 2B). The transformation matrix defines the coordinate transformations from the original coordinate system of the force/torque sensor to that of the CoF/CoR based on the x-y'-z'' convention. To determine the CoR of the canine tooth, which is located approximately in its center of mass, its root was digitally modeled according to the average root-to-crown ratios using specialized software (Autodesk Meshmixer Version 3.5; Autodesk Inc., San Rafael, USA) (Wang et al., 2019). The virtual model of the tooth was matched to the sensor structure in the open-source system MeshLab (Version, 2022.02; Visual Computing Lab of ISTI-CNR University, Italy), so that the center of mass or CoR of the canine could subsequently be calculated using a geometric filter (Cignoni et al., 2008). The calculated transformation parameters were implemented into the control program of ROSS.

The experimental setup utilizes a force control algorithm in its software, where the robot adjusts the tooth position based on forces and moments recorded by the force-torque sensor. Iterative real-time adjustments reduce these forces and moments gradually towards zero, guiding the tooth toward its final position. The movement is divided into a series of small steps, with new force and moment values being recorded before each individual step. The software converts the measured values into appropriate movement vectors, using a compliance matrix based on the mathematical models of Burstone and Christiansen (Burstone and Pryputniewicz, 1980; Christiansen and Burstone, 1969). Depending on the matrix factors and coefficients, the movement pathway varies with respect to the initial rotational or translational components, while the final position remains constant for the same specimen (Fig. 3). The algorithm is based on established tooth movement models and integrates the characteristics of the specific experimental model using the tooth's digitized root surfaces in the different spatial planes as feedback parameters (Nanda, 2005; Burstone, 1985). The algorithm compensates for these differences by applying varying

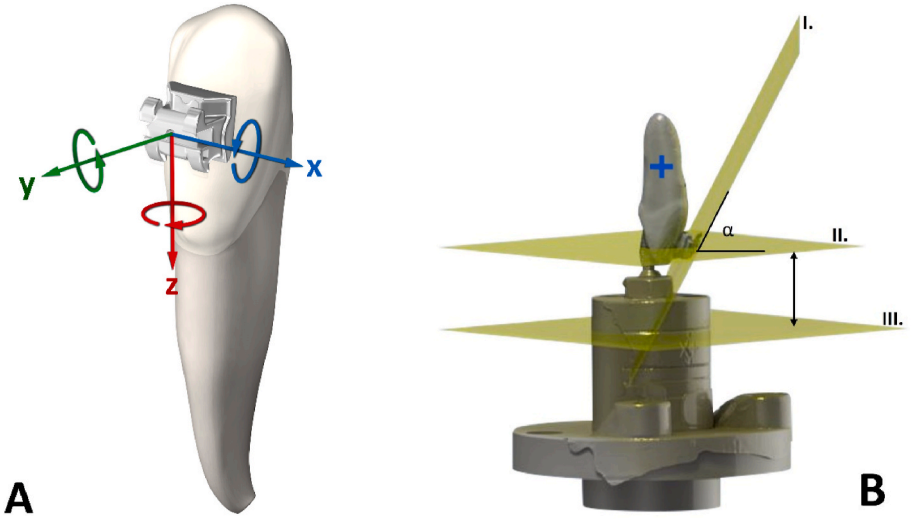

Fig. 2. A: Schematic Representation of the experimental tooth 33, the direction of the measurement components along the x- (mesiodistal), y- (orovestibular) and z- (vertical) axis are shown by the arrows **B:** Partial experimental setup (robot flange, sensor, and tooth structure) generated in Autodesk Inventor with a representation of selected planes I. (vertical plane of at the CoF), II. (horizonal plane of the CoF) and III. (horizontal sensor-plane) and their respective distance and angle in order to geometrically transform the measured values to the CoF (=bracket) and CoR (+).

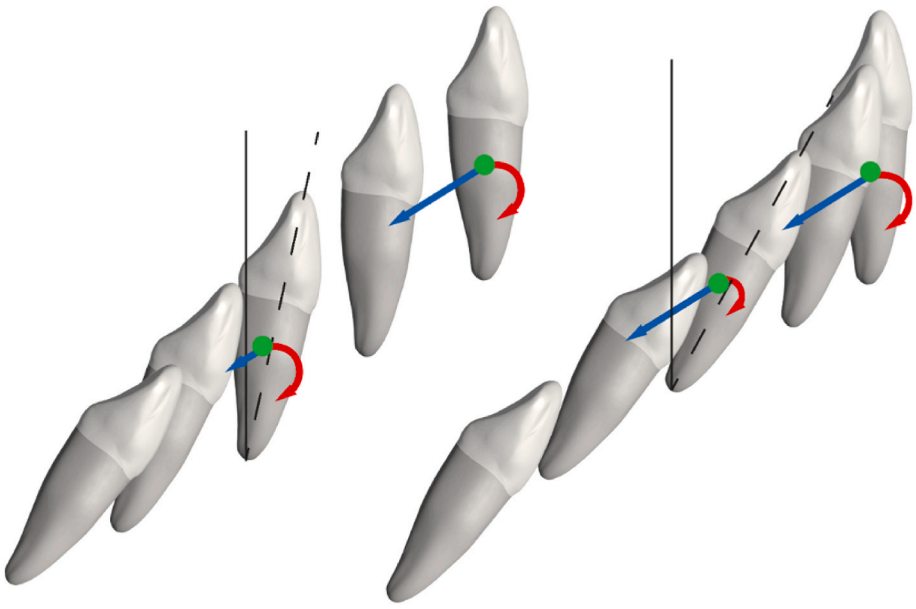

Fig. 3. The compliance matrix determines the ratio of forces to moments in tooth movement. On the left, the pathway shows a more pronounced initial translation than rotation, while on the right, rotation dominates initially. This difference in movement pathways is due to matrix settings, not varying forces or moments, influencing the tooth's translation and rotation balance.

movement amplitudes to balance the forces and moments across the different axes, ensuring that the applied movements are biomechanically appropriate.

The position changes produced no additional forces or moments other than those of the CIS, as the robot moved strictly in the direction of the applied force vectors. An experimental run stopped when the intrusion distance of z = 1.5 mm was achieved.

All samples were manually bent from a 0.017" × 0.025″ β-titanium wire by the same experienced and trained clinician using a template. β-titanium molybdenum alloy was chosen as the material due to its favorable load deflection characteristics and bendability (Schillai and Lehmann, 1989). The design of the CIS was based on literate recommendations and a similar FEM study (Fig. 4A) (Caballero et al., 2015). The distal end of the CIS (1-2) was inserted into the auxiliary tube of the lower left first molar (tooth 36). Adjacent to the auxiliary tube, a 3 mm vertical helical loop (2) and a 35° apically directed tip-back (second order vertical bends) were applied (Fig. 4B). The horizontal segment (3–4) was adapted to the shape of the dental arch and extended mesially to the area of the interproximal contact point between the first premolar (tooth 34) and the canine (tooth 33). At this point (4), a 90° vertical bend towards the occlusal plane was applied. This vertical segment (4–5) of the CIS ended at the upper surface of the canine bracket. Here another 90° horizontal bend was applied mesially, to align the distant end (5–6) of the CIS parallel to the occlusal plane. Activation of the CIS was performed by positioning the distant end on top of the canine bracket.

Three different modifications of the CIS were investigated. Group (#1): unmodified design of the CIS from Fig. 4, which served as the control group for the other experimental groups. In experimental group (#2), a lingually directed toe-in bend (first order horizontal bend) α = 6° was applied into the horizontal segment (3–4) of the CIS (Fig. 5A), in reference to a previous FEM study (Caballero et al., 2015). In group (#3), an additional twist bend (third order bend around the mesio-distal axis) of the vertical segment (4–5) of β = 20° was applied regarding to another FEM study and own biomechanical considerations (Fig. 5B) (Thote et al., 2016). Five CISs of each group (1–3) were examined in independent measurement cycles.

2.3. Statistical analysis

Shapiro-Wilk and Kolmogorov-Smirnov tests were conducted to examine the normative distribution. Since significant ($p < 0.05$) deviations from the assumption of normality distribution were found and due to the small sample size, the Kruskal-Wallis one-way ANOVA was applied as a non-parametric test for independent samples. Consequently post hoc tests were performed, using Bonferroni correction with a significance level of α = 0.05, in order to identify significant differences among the experimental groups ($p < 0.05$). The initial force/moment

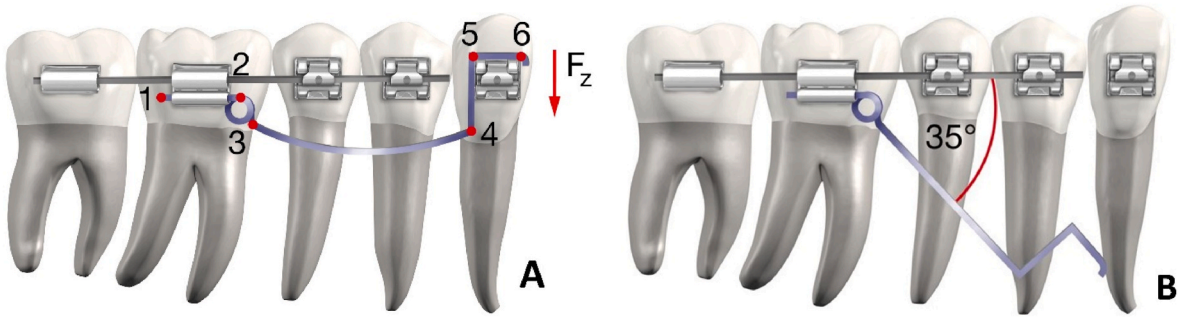

Fig. 4. A: Vestibular aspect of the active CIS showing the different segments (1–6) and the resulting intrusion force (F_z) **B:** Passive CIS with a 35° apical directed tip-back.

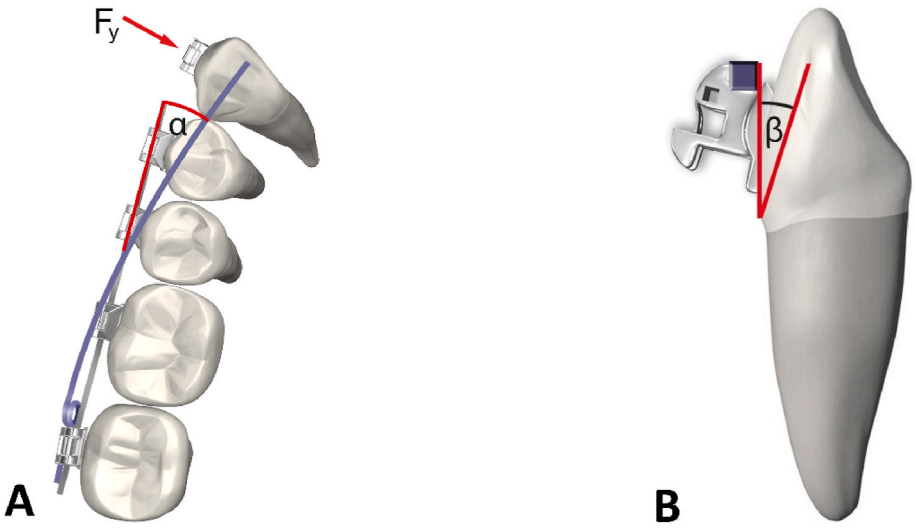

Fig. 5. A: Occlusal aspect of the CIS with a schematic representation of the lingual directed toe-in bend (α) and the resulting orovestibular force (F_y). **B:** Distal aspect of the CIS with a schematic representation of the vertical twist bend (β).

values and realized displacements were analysed by descriptive statistics. All statistical calculations were carried out using IBM SPSS 29 (IBM Corp., Armonk, USA). Graphs were created using OriginPro 2022b (OriginLab Corporation, Northampton, USA).

3. Results

In the experimental setup, the intrusion forces observed initially showed a decreasing trend across the three groups. The average initial intrusion force, uniformly generated by the applied tip-back bend, was recorded at $F_z = 0.31$ N in group (#1), which decreased to $F_z = 0.30$ N in group (#2), and further reduced to $F_z = 0.28$ N in group (#3). The data analysis indicated statistically significant differences ($p < 0.05$) between the force values of group (#1) and group (#3) as outlined in Table 1. Alongside the vertical forces, changes in the horizontal force directions were also significant ($p < 0.05$). The force oriented buccally in group (#1) with $F_y = 0.15$ N and reversed to an oral direction with $F_y = 0.51$ N in group (#3), highlighting significant shifts ($p < 0.05$) as documented in Table 1 and illustrated in Fig. 6A.

Moreover, the moment around the mesiodistal x-axis (M_x) followed a similar pattern. The initial moment for group (#1) was $M_x = 4.63$ Nmm, which decreased to $M_x = 3.56$ Nmm in group (#2) in the buccal direction. In contrast, the initial orientation for group (#3) was significantly different ($p < 0.05$), showing a negative value of $M_x = -1.20$ Nmm, indicating an oral orientation, as depicted in Fig. 6B.

The experimental observations extended to the analysis of the buccal crown tipping tendency. The initial average tipping in group (#1) was $R_x = 2.08°$, which showed a significant reduction ($p < 0.05$) to $R_x = 1.72°$ in group (#2), and a further significant decrease ($p < 0.05$) to only $R_x = 0.05°$ in group (#3), suggesting a stabilization or reduction in tipping over the course of the experiments, as can be seen in Fig. 6C.

Lastly, the displacement along the orovestibular y-axis was assessed. The tooth movement in group (#1) started with a buccal displacement of $y = 0.66$ mm, shifted significantly ($p < 0.05$) to a negative displacement of −0.29 mm in group (#2), and further moved to a significantly ($p < 0.05$) larger negative displacement of −1.47 mm orally in group (#3). These movements are documented in Table 1 and visualized in Fig. 6D, indicating a clear trend of oral movement across the experimental groups.

In summary, the respective impacts of the introduced bends and modifications of the CIS can be described as follows. The baseline modification (#1) resulted in a significant buccal tipping and transverse displacement of the tooth towards the vestibular direction, in addition to the intended intrusion movement. The toe-in bend (#2) reduced the buccal tipping of the tooth and changed the transverse displacement from initially vestibular to a slight oral shift. The additional twist bend (#3) nearly eliminated the buccal tipping but resulted in a significant oral displacement of the canine.

4. Discussion

The objective of this study was the biomechanical investigation of mandibular canine intrusion using segmented-arch mechanics, specifically CIS. For the first time the novel Robot Orthodontic Measurement & Simulation System (ROSS) was utilized to automatically and dynamically measure the forces and moments during the segmented intrusion of a mandibular canine, providing unprecedented precision and real-time data analysis without manual intervention. The effects and the side effects of various additional bends or modifications of the CIS on the resulting forces and moments during canine intrusion were examined, in particular to determine the modification that allows for intrusion with minimal collateral forces and moments to avoid adverse tooth

Table 1
Means, maximum values (Max.), and respective standard deviations (SD) of the initial intrusion forces F_z [N], the initial orovestibular forces F_y [N], the initial protrusion moments M_x [Nmm], orovestibular crown-tipping R_x [°] and realized orovestibular displacement y [mm] for the different CIS groups (#1,#2,#3). Significant differences between the groups' values are indicated by the same superscript letters (^{1,2,3}). Kruskal-Wallis one-way ANOVA with post hoc test including correction according to Bonferroni were performed to determine these differences, with a significance level set at $p < 0.05$.

Cantilver-Modification		F_z [N]		F_y [N]		M_x [Nmm]		R_x [°]		y [mm]	
		Mean (SD)	Max.	Mean (SD)	Max.	Mean (SD)	Max.	Mean (SD)	Max.	Mean (SD)	Max.
1	0° Toe-In	0.31^{3} (±0.01)	0.33	$0.15^{2,3}$ (±0.01)	0.16	$4.63^{2,3}$ (±0.19)	4.91	$2.08^{2,3}$ (±0.02)	2.11	$0.66^{2,3}$ (±0.02)	0.69
2	6° Toe-In	0.30 (±0.01)	0.30	$-0.10^{1,3}$ (±0.05)	−0.15	$3.56^{1,3}$ (±0.18)	3.91	$1.72^{1,3}$ (±0.05)	1.77	$-0.29^{1,3}$ (±0.07)	−0.37
3	6° Toe-In + 20° Twist	0.28^{1} (±0.02)	0.31	$-0.47^{1,2}$ (±0.02)	−0.51	$-1.20^{1,2}$ (±0.23)	−1.54	$0.05^{1,2}$ (±0.02)	0.07	$-1.47^{1,2}$ (±0.02)	−1.49

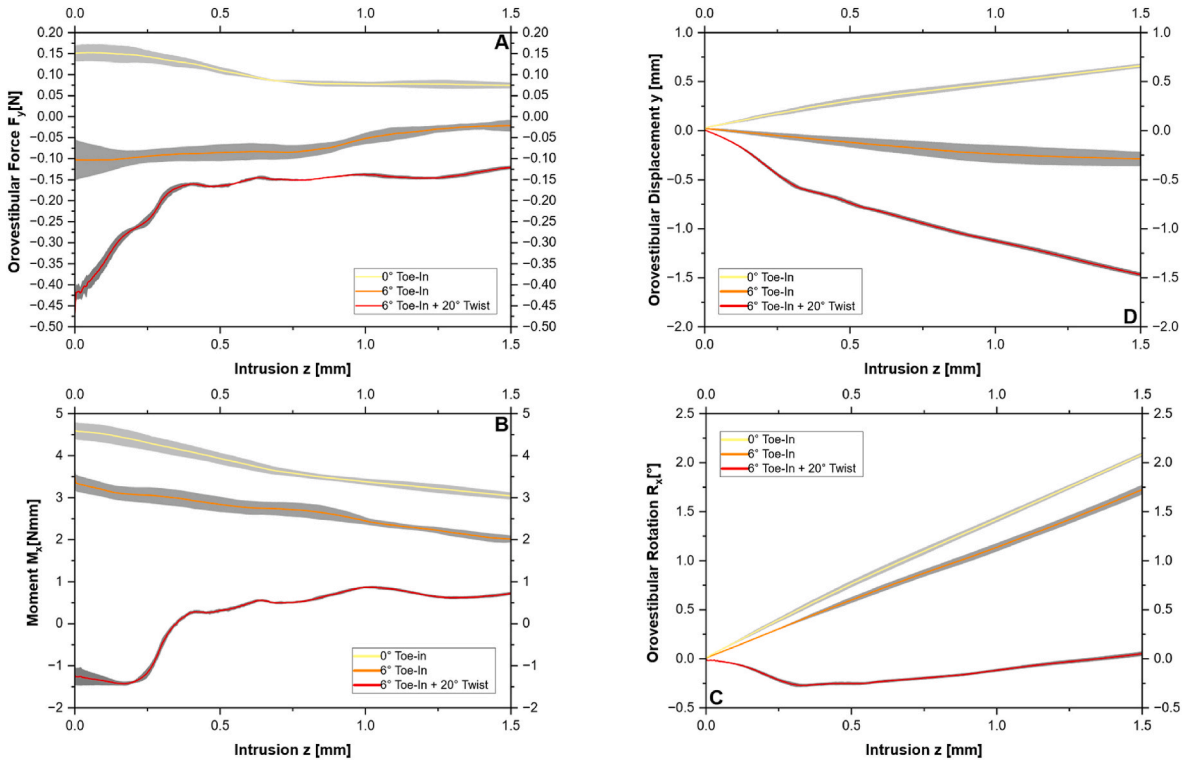

Fig. 6. A: Correlation between orovestibular force [F_y] and intrusion distance [z] **B:** Correlation between orovestibular moment [M_x] and intrusion distance [z] **C:** Correlation between buccal crown-tipping [R_x] and intrusion distance [z] **D:** Correlation between orovestibular displacement [y] and intrusion distance [z] - Shown are the averaged curves of each CIS group with a graphically visualized standard deviation range.

movements.

The intrusion of canines is a common clinical challenge in the treatment of deep bites malocclusions. In fixed orthodontic treatment, CIS allow applying intrusive forces on the canines without transmitting extruding forces to the incisors, which would be a side effect in case of using continuous archwires. Extrusion of the incisors should be avoided in order not to increase the overbite and thus aggravate the deep bite. In the literature, β-titanium springs with loop and tip-back bends are proposed for this indication (Bilinska et al., 2022; Elkholy et al., 2023). Applying a vertical force with buccal fixed appliances vestibular of the CoR will create a corresponding torsional moment and thus vestibular tipping of the tooth. In an FEM study, Caballero et al. found that adding a toe-in bend of 6° was suitable to counterbalance this tipping moment and thus pure intrusion was achieved in their simulation. Thote et al. investigated the use of CIS using lingual fixed appliances in another FEM model and found that the application of a vertical toe-bend or twist is necessary for certain canine inclinations (Thote et al., 2016).

In contrast to the results of the available FEM studies, the results of the present study showed that pure intrusion of the canine was not achieved, irrespective of the modifications applied. The addition of compensatory bends reduced or eliminated the vestibular tipping moment, however other collateral forces and moments were generated as a result as can be seen in Fig. 6. This is in line with biomechanical considerations, since applying toe-in bends from vestibular will result in a lingual translational movement that is not compensated, even if both rotational moments would completely counterbalance each other. According to the fourth Newtonian axiom or the principle of superposition, individual forces acting on the same point of a body can be combined via vector addition in order to form a resulting total force (Gross et al., 2019; Newton, 2020). Thus, a pure intrusion is only possible if the corresponding force vector passes through the CoR of the tooth (Burstone, 1985; Sander et al., 2011; Wichelhaus, 2013) and all acting moments are compensated for by counter moments (Fig. 7c). With buccal fixed appliances, to achieve pure intrusion, the additional horizontal force

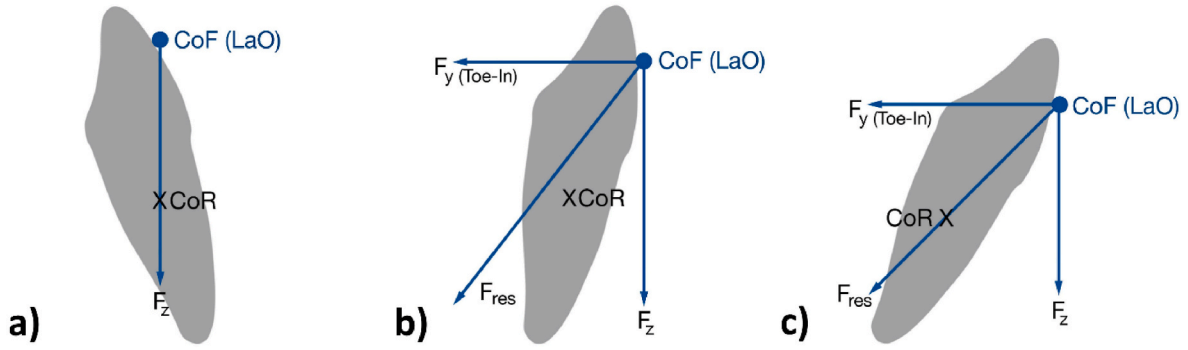

Fig. 7. Schematic representation of the impact of the oro-vestibular inclination of the canine on the intrusion movement. **a):** Lingual tipped canine. **b):** Normal inclinated canine. **c):** Labial tipped canine.

component would need to completely counterbalance the vestibular tipping moment and the sum vector of forces would need to pass through the CoR (Liang et al., 2009). As illustrated in Fig. 7, this scenario would require a significant initial oro-vestibular inclination of the canine (Fig. 7c). The physiologic inclination of lower canines usually ranges between −9° and +9° (Andrews, 1972; Vardimon and Lambertz, 1986)). Hence, this scenario is unlikely to occur in biomechanical terms (Fig. 7b). In conclusion, it can be said that due to the variable inclination of a canine tooth, it is challenging to make a uniform statement regarding the correct CIS modification. It always requires an individual assessment of the initial situation, as in some cases an unphysiologically high vertical (F_z) or horizontal (F_y) force component would be necessary to achieve pure intrusion through the CoR or whether a toe-in or toe out bend is needed or not (Fig. 7a).

Another finding noted was that the orovestibular moment (M_x) and the resulting rotation (R_x) leading to buccal crown tipping of the canine, decreased with the introduction of a compensatory 6° toe-in bend, from an average of 4.63 Nmm to 3.56 Nmm and from 2.08° to 1.72°. Only with an additional 20° twist bend in the vertical section of the intrusion springs the buccal tipping moment was decreased to approximately zero, with a maximum R_x of 0.07°. The applied twist bends produced an intrusive and a horizontal force component. However, simultaneously, an increasing displacement of the tooth towards lingual was observed. While the canine in the control group, without any additional bends, moved an average of 0.66 mm buccally by the completion of intrusion, this movement reversed in the group with compensatory toe-in bend, reaching an oral displacement of an average of 0.29 mm. Applying toe-in and twist bends to fully counteract the vestibular tipping moment, the displacement reached even higher values, up to 1.49 mm orally.

Summarizing the key findings, the results of the performed biomechanical simulations suggest that pure canine intrusion can only be achieved in specific treatment scenarios depending on the inclination of the canine. Individual adjustment of the compensatory bends is crucial in this process. Although the 6° toe-in bend in group (#2) led to an oral displacement, it remains the recommended modification in view of the minor extent of this effect. Also, from an aesthetic perspective, a slight tipping of the canines should be preferred over a considerable horizontal displacement (Jenny and Cons, 1996; Kalia, 2020).

The intrusive force (F_z) in the CIS group without additional bends (#1), initial forces averaged 0.31 N, comparable to the force range in the reference study (Caballero et al., 2015). Since the force during an axial or vertical tooth movement like intrusion is only distributed over approximately 10% of the total root surface, even forces of 0.3–0.5 N may already cause root resorptions (Sander et al., 2011; Wichelhaus, 2013; Kurol and Owman-Moll, 1998). Due to the fact that, during simulated intrusions, a larger portion of the root surface was loaded due to the occurring tipping (R_x) and orovestibular displacement, the activation of β-titanium intrusion springs with a helical loop of 3 mm and 35° tip-back seems justifiable (Proffit et al., 2007; Ricketts, 1976; Reitan, 1985). In the other CIS groups (#2,#3) the application of bends reduced initial intrusive force values despite the uniform activation using a 35° tip-back. This can be explained by the fact that the additional bends (toe-in/twist) affect the apically directed intrusion force due to changes in the orovestibular force (F_y) and orovestibular torque-moment (M_x).

It should be noted that the direct transferability of results from biomechanical studies to clinical scenarios is limited (Drescher et al., 1991; Badawi et al., 2009; Sifakakis and Eliades, 2017). The simulations did not account for the behaviour and the characteristics of the periodontal ligament and the alveolar bone or the complexity of individual movement phases, where the velocity of tooth movement may vary. The presented methodology relied on biomechanical aspects, such as the CoF, the CoR and constant force and moment reduction which were considered as part of the force-control algorithm of the experimental setup (Li et al., 2018, 2021a). Although the comparability between FEM and instrument based in vitro studies is limited, the overall good agreement with regard to the force and moment ranges in the reference FEM studies with a simulated PDL and alveolar bone tissue underlines that the provided assumptions appear plausible (Cicciu, 2020; Cervino et al., 2020; Romanyk et al., 2020). Clinically, the CoR has been observed to dynamically change during clinical orthodontic tooth movement, whereas the CoR and CoF were set to static values in the experimental setup given the lack of quantitative evidence for this effect (Wichelhaus, 2013; Schmidt et al., 2016). In addition, the posterior segment, where the CIS was inserted into the molar attachment, was fixed, simulating a maximum anchorage case. Clinically tooth mobility would persist, even if teeth are joined into a unit e.g. with figure-8 steel ligatures, so that a certain portion of the applied forces and moments are distributed to the respective teeth (Frias Cortez et al., 2022). Therefore, the simulated situation corresponds to the clinical use of intraosseous anchorage devices, which was shown to provide maximum anchorage and effectively prevent tooth movement (Liu et al., 2020). Due to the comparatively larger root surface and thus higher anchorage capacity of a molar in occlusion, a comparatively low side effect can also be assumed in other anchorage situations. The experimental environment did not account for the presence of saliva, which can alter frictional phenomena and, consequently, the outcomes of the measurements (Li et al., 2021b; Kusy and Whitley, 2003). Lastly, the manual adjustment of the CISs is prone to variability. Despite being carried out by an experienced clinician, there is a certain deviation between the individual CISs, as indicated by the graphically illustrated standard deviation in Fig. 6. Exact reproducibility through manual bending techniques is unrealistic, and individual robot-assisted manufacturing of archwires is not yet advanced for such mechanics and has not been verified in any literature. Due to this the observed variability reflects the clinical use of archwire bends, inherently associated with a certain level of imprecision, which is likely even more pronounced in everyday clinical practice.

Within its limitations the study provides a detailed analysis of the forces and moments in segmented canine intrusion using CIS. The CIS with a 6° toe-in bend (modification #2) significantly reduces vestibular crown tipping, offering a balance between intrusive forces and minimal collateral effects. These findings guide clinicians in selecting suitable CIS modifications based on canine inclination. The Robot Orthodontic Measurement & Simulation System allowed precise control and validation of orthodontic forces, reinforcing its research applicability. Importantly, physical test samples corroborated existing FEM research, critically refuting claims of pure intrusion feasibility. The detailed biomechanical data and limitations identified, support further investigation into alternative CISdesigns and their in vivo performance.

5. Conclusions

TMA CISs with 3 mm vertical loops and 35° tip-back bends produced suitable force ranges for canine intrusion. All configurations investigated were associated with collateral forces and moments, in particular in the horizontal plane. The vestibular tipping moment observed in the unmodified group (#1) was decreased to a lower degree by applying a 6° toe-in bend (#2). An additional 20° twist bend (#3) counterbalanced the vestibular tipping moment but resulted in significant oral displacement. Within the limitations of this study, modification (#2) can be recommended for clinical application regarding the biomechanical findings.

Funding

This research did not receive any specific grant from funding agencies in the public, commercial, or not-for-profit sector.

CRediT authorship contribution statement

Hisham Sabbagh: Writing – original draft, Methodology, Investigation, Conceptualization. **Benedikt Dotzer:** Writing – original draft, Software, Investigation, Formal analysis. **Uwe Baumert:** Writing –

review & editing, Software, Data curation. **Linus Hötzel:** Writing – review & editing, Visualization, Software, Methodology. **Corinna Lesley Seidel:** Writing – review & editing, Validation. **Andrea Wichelhaus:** Validation, Supervision, Resources.

Declaration of competing interest

Have no conflict of interest to disclose.

Data availability

Data will be made available on request.

Acknowledgements

Not applicable.

References

Abu Arqub, S., Al-Moghrabi, D., Iverson, M.G., Farha, P., Alsalman, H.A., Uribe, F., 2023. Assessment of the efficacy of various maxillary molar intrusion therapies: a systematic review. Prog. Orthod. 24, 37.

Agrawal, G., 2016. Deep bite its etiology, diagnosis and management: a review. J. Orthod. 2, 12.

Al-Buraiki, H., Sadowsky, C., Schneider, B., 2005. The effectiveness and long-term stability of overbite correction with incisor intrusion mechanics. Am. J. Orthod. Dentofacial Orthop. 127, 47–55.

Alhammadi, M.S., Halboub, E., Fayed, M.S., Labib, A., El-Saaidi, C., 2018. Global distribution of malocclusion traits: a systematic review. Dental press journal of orthodontics 23, 40. e1-. e10.

Andrews, L.F., 1972. The six keys to normal occlusion. Am. J. Orthod. 62, 296–309.

Baccetti, T., Franchi, L., Giuntini, V., Masucci, C., Vangelisti, A., Defraia, E., 2012. Early vs late orthodontic treatment of deepbite: a prospective clinical trial in growing subjects. Am. J. Orthod. Dentofacial Orthop. 142, 75–82.

Badawi, H.M., Toogood, R.W., Carey, J.P., Heo, G., Major, P.W., 2009. Three-dimensional orthodontic force measurements. Am. J. Orthod. Dentofacial Orthop. 136, 518–528.

Bilinska, M., Kristensen, K.D., Dalstra, M., 2022. Cantilevers: multi-tool in orthodontic treatment. Dent. J. 10, 135.

Burstone, C.J., 1966. The mechanics of the segmented arch techniques. Angle Orthod. 36, 99–120.

Burstone, C.R., 1977. Deep Overbite Correction by Intrusion, vol. 72. Am J Orthod, pp. 1–22.

Burstone, C.J., 1985. Application of bioengineering to clinical orthodontics. Orthodontics: Current Principles and Techniques, pp. 154–186.

Burstone, C.J., Pryputniewicz, R.J., 1980. Holographic determination of centers of rotation produced by orthodontic forces. Am. J. Orthod. 77, 396–409.

Caballero, G.M., Carvalho Filho, O.A., Hargreaves, B.O., Brito, H.H., Magalhaes Junior, P.A., Oliveira, D.D., 2015. Mandibular canine intrusion with the segmented arch technique: a finite element method study. Am. J. Orthod. Dentofacial Orthop. 147, 691–697.

Cervino, G., Fiorillo, L., Arzukanyan, A.V., Spagnuolo, G., Campagna, P., Cicciu, M., 2020. Application of bioengineering devices for stress evaluation in dentistry: the last 10 years FEM parametric analysis of outcomes and current trends. Minerva Stomatol. 69, 55–62.

Christiansen, R.L., Burstone, C.J., 1969. Centers of rotation within the periodontal space. Am. J. Orthod. 55, 353–369.

Cicciu, M., 2020. Bioengineering methods of analysis and medical devices: a current trends and state of the art. Materials 13.

Cignoni, P., Callieri, M., Corsini, M., Dellepiane, M., Ganovelli, F., Ranzuglia, G., 2008. Meshlab: an open-source mesh processing tool. Eurographics Italian Chapter Conference: Salerno, Italy, pp. 129–136.

Dotzer, B., Stocker, T., Wichelhaus, A., Janjic Rankovic, M., Sabbagh, H., 2023. Biomechanical simulation of forces and moments of initial orthodontic tooth movement in dependence on the used archwire system by ROSS (Robot Orthodontic Measurement & Simulation System). J. Mech. Behav. Biomed. Mater. 144, 105960.

Drescher, D., Bourauel, C., Thier, M., 1991. Application of the orthodontic measurement and simulation system (OMSS) in orthodontics. Eur. J. Orthod. 13, 169–178.

Elkholy, F., Wulf, S., Jäger, R., Schmidt, F., Lapatki, B.G., 2023. Mechanical loads exerted by different configurations of Burstone's 3-piece segmented mechanics during a simulated intrusion of the mandibular incisors. Am. J. Orthod. Dentofacial Orthop. 164 (1), 106–115.

Frias Cortez, M.A., Bourauel, C., Reichert, C., Jäger, A., Reimann, S., 2022. Numerical and biomechanical analysis of orthodontic treatment of recovered periodontally compromised patients. Journal of Orofacial Orthopedics/Fortschritte der Kieferorthopadie. 83.

Ghafari, J.G., Macari, A.T., Haddad, R.V., 2013. Deep bite: treatment options and challenges. Semin Orthod. Elsevier, pp. 253–266.

Gross, D., Hauger, W., Schröder, J., Wall, W.A., Gross, D., Hauger, W., et al., 2019. Kräfte mit gemeinsamem Angriffspunkt. Tech. Mech. 1, 15–41. Statik.

Jenny, J., Cons, N.C., 1996. Establishing malocclusion severity levels on the Dental Aesthetic Index (DAI) scale. Aust. Dent. J. 41, 43–46.

Kalia, R., 2020. An analysis of the aesthetic proportions of anterior maxillary teeth in a UK population. Br. Dent. J. 228, 449–455.

Kamble, R.H., Lohkare, S., Hararey, P.V., Mundada, R.D., 2012. Stress distribution pattern in a root of maxillary central incisor having various root morphologies: a finite element study. Angle Orthod. 82, 799–805.

Kurol, J., Owman-Moll, P., 1998. Hyalinization and root resorption during early orthodontic tooth movement in adolescents. Angle Orthod. 68, 161–166.

Kusy, R.P., Whitley, J.Q., 2003. Influence of fluid media on the frictional coefficients in orthodontic sliding. Semin Orthod. Elsevier, pp. 281–289.

Li, Y., Jacox, L.A., Little, S.H., Ko, C.-C., 2018. Orthodontic tooth movement: the biology and clinical implications. The Kaohsiung journal of medical sciences 34, 207–214.

Li, Y., Zhan, Q., Bao, M., Yi, J., Li, Y., 2021a. Biomechanical and biological responses of periodontium in orthodontic tooth movement: up-date in a new decade. Int. J. Oral Sci. 13, 20.

Li, H., Stocker, T., Bamidis, E.P., Sabbagh, H., Baumert, U., Mertmann, M., et al., 2021b. Effect of different media on frictional forces between tribological systems made from self-ligating brackets in combination with different stainless steel wire dimensions. Dent. Mater. J. 40, 1250–1256.

Liang, W., Rong, Q., Lin, J., Xu, B., 2009. Torque control of the maxillary incisors in lingual and labial orthodontics: a 3-dimensional finite element analysis. Am. J. Orthod. Dentofacial Orthop. 135, 316–322.

Liu, Y., Yang, Z-j, Zhou, J., Xiong, P., Wang, Q., Yang, Y., et al., 2020. Comparison of anchorage efficiency of orthodontic mini-implant and conventional anchorage reinforcement in patients requiring maximum orthodontic anchorage: a systematic review and meta-analysis. J. Evid. Base Dent. Pract. 20, 101401.

Luchian, I., Martu, M.-A., Tatarciuc, M., Scutariu, M.M., Ioanid, N., Pasarin, L., et al., 2021. Using fem to assess the effect of orthodontic forces on affected periodontium. Appl. Sci. 11, 7183.

Nanda, R., 2005. Biomechanics and Esthetic Strategies in Clinical Orthodontics. Elsevier Health Sciences.

Nanda, R., Kuhlberg, A., 2007. Treatment of Overbite Malocclusion: Biomechanical and Esthetic Strategies in the Orthodontic Clinic. Santos.

Newton, I., 2020. The mathematical principles of natural philosophy. Definitions, Scholium, para 9, 1686.

Otto, R.L., Anholm, J.M., Engel, G.A., 1980. A comparative analysis of intrusion of incisor teeth achieved in adults and children according to facial type. Am. J. Orthod. 77, 437–446.

Parker, C.D., Nanda, R.S., Currier, G.F., 1995. Skeletal and dental changes associated with the treatment of deep bite malocclusion. Am. J. Orthod. Dentofacial Orthop. 107, 382–393.

Proffit, W.R., Fields, Jr HW., Sarver, D.M., 2007. Contemporary Orthodontics, fourth ed. ed. Elsevier Health Sciences, St. Louis.

Reitan, K., 1985. Biological principles and reactions. Orthodontics, Current Orthodontic Concepts and Techniques, pp. 141–142.

Ricketts, R.M., 1976. Bioprogressive therapy as an answer to orthodontic needs. Part II. Am. J. Orthod. 70, 359–397.

Ricketts, R., Bench, R., Gugino, C., Hilgers, J., Schulhof, R., 1979. Mechanics sequence for class II division I cases. Bioprogresive Therapy Ricketts RM (ed): Rocky Mountain Orthodontics 169–181. Denver, CO.

Romanyk, D.L., Vafaeian, B., Addison, O., Adeeb, S., 2020. The use of finite element analysis in dentistry and orthodontics: critical points for model development and interpreting results. Semin Orthod. Elsevier, pp. 162–173.

Sander, F.G., Ehrenfeld, M., Schwenzer, N., 2011. Zahn-Mund-Kiefer-Heilkunde Kieferorthopädie. Georg Thieme Verlag KG, Stuttgart.

Sankey, W.L., Buschang, P.H., English, J., Owen 3rd, A.H., 2000. Early treatment of vertical skeletal dysplasia: the hyperdivergent phenotype. Am. J. Orthod. Dentofacial Orthop. 118, 317–327.

Schillai, G., Lehmann, K., 1989. Untersuchung über die Beziehung zwischen Aktivierungskraft und Auslenkung bei verschiedenen Zahnzugfedern (Closing-Loops). Fortschr. Kieferorthop. 50, 172–178.

Schmidt, F., Geiger, M.E., Jäger, R., Lapatki, B.G., 2016. Comparison of methods to determine the centre of resistance of teeth. Comput. Methods Biomech. Biomed. Eng. 19, 1673–1682.

Sifakakis, I., Eliades, T., 2017. Laboratory evaluation of orthodontic biomechanics: the clinical applications revisited. Semin Orthod. Elsevier, pp. 382–389.

Singh, J.R., Kambalyal, P., Jain, M., Khandelwal, P., 2016. Revolution in orthodontics: finite element analysis. J. Int. Soc. Prev. Community Dent. 6, 110–114.

Thote, A.M., Uddanwadiker, R.V., Sharma, K., Shrivastava, S., 2016. Optimum force system for intrusion and extrusion of maxillary central incisor in labial and lingual orthodontics. Comput. Biol. Med. 69, 112–119.

Thote, A.M., Sharma, K., Uddanwadiker, R.V., Shrivastava, S., 2017a. Optimum pure intrusion of a mandibular canine with the segmented arch in lingual orthodontics. Bio Med. Mater. Eng. 28, 247–256.

Thote, A.M., Sharma, K., Uddanwadiker, R.V., Shrivastava, S., 2017b. Pure intrusion of a mandibular canine with segmented arch in lingual orthodontics: a numerical study with 3-dimensional finite element analysis. Biocybern. Biomed. Eng. 37, 590–598.

Vardimon, A.D., Lambertz, W., 1986. Statistical evaluation of torque angles in reference to straight-wire appliance (SWA) theories. Am. J. Orthod. 89, 56–66.

Wang, J., Rousso, C., Christensen, B.I., Li, P., Kau, C.H., MacDougall, M., et al., 2019. Ethnic differences in the root to crown ratios of the permanent dentition. Orthod. Craniofac. Res. 22, 99–104.

Wanjun, Z., Jinyuan, L., Yongping, M., Linqing, G., 2015. The development of orthodontics in the three dimensional finite element method. Journal of Hebei Medical College for Continuing Education 32, 75.

Wichelhaus, A., 2013. Kieferorthopädie - Therapie Band 1: Farbatlanten der Zahnmedizin. Stuttgart Georg Thieme Verlag.
Wichelhaus, A., Hüffmeier, S., Sander, F.-G., 2003. Dynamic functional ForceMeasurements on an anterior bite plane during theNight. Journal of Orofacial Orthopedics/Fortschritte der Kieferorthopädie 64, 417–425.
Zeno, K.G., Ammoury, M.J., 2023. The Surge of Finite Element Analysis in the Study of Orthodontic Mechanics: Are the Findings Applicable in Practice? Semin Orthod. Elsevier.